THREE-DIMENSIONAL EUTROPHICATION MODEL OF CHESAPEAKE BAY

By Carl F. Cerco,[1] Associate Member, ASCE, and Thomas Cole[2]

ABSTRACT: CE-QUAL-ICM is a three-dimensional, time-variable, eutrophication model. CE-QUAL-ICM incorporates 22 state variables that include physical properties; multiple forms of algae, carbon, nitrogen, phosphorus, and silica; and dissolved oxygen. The model is part of a larger package that includes a three-dimensional hydrodynamic model and a benthic-sediment diagenesis model. Application to Chesapeake Bay over a three-year period, 1984–86, indicates the model successfully simulates water-column and sediment processes that affect water quality. Phenomena simulated include formation of the spring algal bloom subsequent to the annual peak in nutrient runoff, onset and breakup of summer anoxia, and coupling of organic particle deposition with sediment-water nutrient and oxygen fluxes. The study demonstrates that complex eutrophication problems can be addressed with coupled three-dimensional hydrodynamic and water-quality models.

INTRODUCTION

Chesapeake Bay is our nation's largest and most productive estuary. The bay is plagued with problems that accompany agricultural and industrial development and population growth along its shores and headwaters. Many of these problems, including bottom-water anoxia, decline in fisheries, and loss of submerged aquatic vegetation, are associated with eutrophication of the bay.

Specifications for a three-dimensional, state-of-the-art model package required to address eutrophication issues in the bay were developed in four technical workshops (HydroQual 1988). The workshops called for a model with abilities to:

1. Project response of water column and benthic sediments to management activities
2. Perform short-term (annual) and long-term (decades) simulations
3. Determine effect of spring runoff events on summer anoxia
4. Address lateral variations in water quality
5. Determine response of bay to area-specific nutrient control strategies
6. Predict the response time of the bay to management actions
7. Evaluate frequency of critical water-quality events
8. Evaluate historical changes in anoxia

This paper is one of a series that describe fulfillment of the workshop goals. Formulation of the eutrophication component of the Chesapeake Bay model package (CBMP) and its interactions with other models in the package are described. The capability of the model to simulate crucial elements

[1]Res. Hydrol., Mail Stop ES-Q, USACE Waterways Experiment Station, 3909 Halls Ferry Road, Vicksburg, MS 39180.

[2]Res. Hydrol., Mail Stop ES-Q, USACE Waterways Experiment Station, 3909 Halls Ferry Road, Vicksburg, MS.

Note. Discussion open until May 1, 1994. To extend the closing date one month, a written request must be filed with the ASCE Manager of Journals. The manuscript for this paper was submitted for review and possible publication on May 19, 1992. This paper is part of the ***Journal of Environmental Engineering***, Vol. 119, No. 6, November/December, 1993. ©ASCE, ISSN 0733-9372/93/0006-1006/$1.00 + $.15 per page. Paper No. 4083.

of the eutrophication process is demonstrated. Subsequent papers will evaluate historical changes in anoxia and illustrate the time scale and nature of the bay response to management actions.

CHESAPEAKE BAY MODEL PACKAGE

Transport Processes

The CBMP consists of three models and linkages between them. Transport processes are modeled by the curvilinear hydrodynamics in three dimensions—Waterways Experiment Station (CH3D-WES) model (Johnson et al. 1993). CH3D-WES produces three-dimensional predictions of velocity, diffusion, surface elevation, salinity, and temperature on an intratidal (≈5 min) time scale. Appended to CH3D-WES is a Lagrangian processor (Dortch et al. 1992) that filters intratidal details from hydrodynamic output but maintains intertidal (≈12 h) transport. Intertidal flow, vertical diffusion, and surface elevation are written to a disk for use as input to the eutrophication model.

Water Quality

Water quality is modeled by an integrated-compartment model, CE-QUAL-ICM, developed for the present study. The compartment structure provides flexibility for coupling CE-QUAL-ICM with alternate hydrodynamic models. CE-QUAL-ICM solves, for each grid cell and for each state variable, the conservation of mass equation:

$$\frac{\delta V_i C_i}{\delta t} = \sum_{j=1}^{n} Q_j C_j^* + \sum_{j=1}^{n} A_j D_j \frac{\delta C}{\delta x_j} + \sum S_i \quad \ldots\ldots\ldots\ldots\ldots\ldots\ldots\ldots (1)$$

in which: V_i = volume of ith compartment; C_i = concentration in ith compartment; Q_j = volumetric flow across flow face j of ith compartment; C_j^* = concentration in flow across flow face j; A_j = area of flow face j; D_j = diffusion coefficient at flow face j; n = number of flow faces attached to ith compartment; S_i = external loads and kinetic sources and sinks in ith compartment; and t, x = temporal and spatial coordinates. Finite-difference solution to (1) employs the QUICKEST algorithm (Leonard 1979) in the horizontal directions and a Crank-Nicolson scheme in the vertical direction.

CE-QUAL-ICM incorporates 22 state variables (Table 1). Kinetic interactions among the state variables are described in 80 partial differential equations (Cerco and Cole 1993) that employ over 140 parameters. The state variables can be categorized into six groups or cycles. The physical group consists of salinity, temperature, and inorganic suspended solids. Salinity is included primarily to verify the linkage to CH3D-WES. When the models are properly linked, salinity predicted by CE-QUAL-ICM replicates predictions by CH3D-WES. Temperature, predicted by an equilibrium-temperature approach (Edinger et al. 1974), is included for its fundamental impact on the rate of biochemical processes. In the present model configuration, inorganic solids are a surrogate for iron and manganese that adsorb phosphate (PO_4) and dissolved silica (DSil) in the water column.

The simulated carbon cycle (Fig. 1) originates with carbon fixation by three algal groups. A portion of the algal carbon is lost as CO_2 through respiration. Additional algal carbon is converted to dissolved organic carbon (DOC) or particulate organic carbon through algal mortality and predation. Two particulate carbon groups, labile particulate organic carbon (LPOC)

TABLE 1. CE-QUAL-ICM State Variables

Variable (1)	Variable (2)
Temperature	Dissolved organic nitrogen
Salinity	Labile particulate organic nitrogen
Inorganic suspended solids	Refractory particulate organic nitrogen
Diatoms	Total phosphate
Cyanobacteria (blue-green algae)	Dissolved organic phosphorus
Other phytoplankton	Labile particulate organic phosphorus
Dissolved organic carbon	Refractory particulate organic phosphorus
Labile particulate organic carbon	Dissolved oxygen
Refractory particulate organic carbon	Chemical oxygen demand
Ammonium	Dissolved silica
Nitrate + nitrite	Particulate biogenic silica

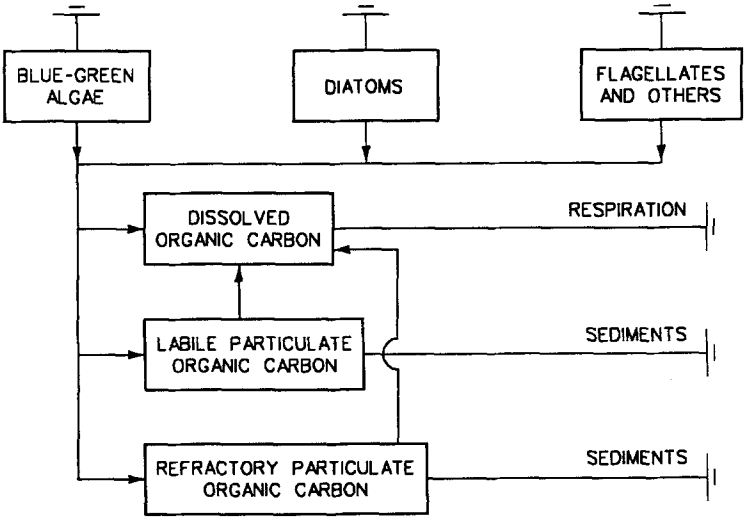

FIG. 1. Simulated Carbon Cycle

and refractory particulate organic carbon (RPOC), are included to reflect the differential rates at which organic matter decomposes. A fraction of the particulate carbon is hydrolyzed to DOC. DOC produced directly by algae or through by hydrolysis is removed from the system through heterotrophic respiration. The balance of the particulate and algal carbon settles to the bottom where it is incorporated into the sediments.

In the simulated nitrogen cycle (Fig. 2), nitrate-nitrite (NO_3), and ammonium (NH_4) are incorporated by the three algal groups. Mortality and predation return algal nitrogen to the water column as dissolved organic nitrogen (DON), labile (LPON) and refractory particulate organic nitrogen (RPON), and as NH_4. Hydrolysis converts a portion of the particulate nitrogen to DON. The remainder settles into the benthic sediments along with the nitrogen incorporated in the biomass of settled algae. DON is mineralized to NH_4 and rendered available again to the algae either as NH_4 or as NO_3 produced by nitrification.

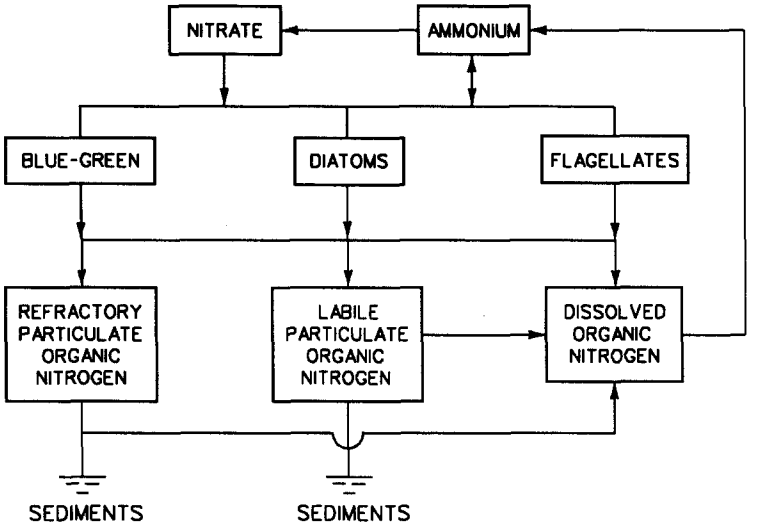

FIG. 2. Simulated Nitrogen Cycle

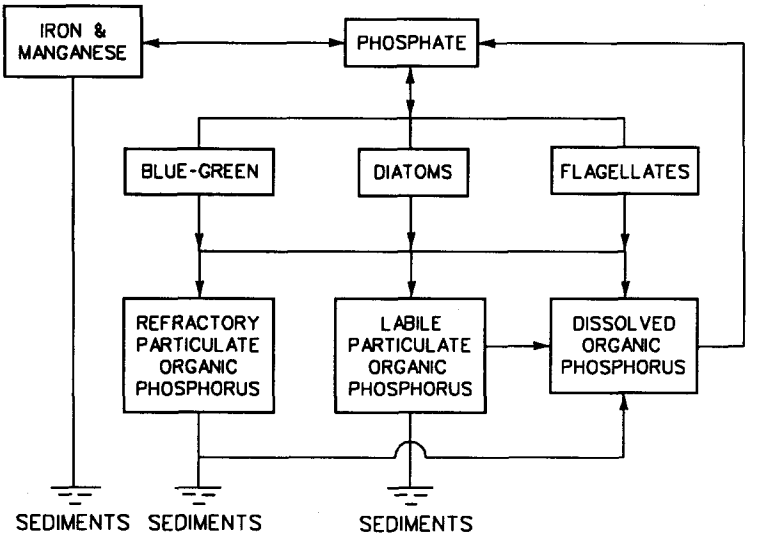

FIG. 3. Simulated Phosphorus Cycle

In the simulated phosphorus cycle (Fig. 3), PO_4 is incorporated by three algal groups. Algal phosphorus is returned to the water column as dissolved organic phosphorus (DOP), labile and refractory particulate organic phosphorus (LPOP and RPOP, respectively), and as PO_4. A portion of the particulate phosphorus is hydrolyzed to DOP. The balance is lost to the sediments along with phosphorus incorporated in settled algae. DOP is mineralized to PO_4 and made available again to the algae. PO_4 also undergoes sorption-desorption with iron and manganese particles. This process

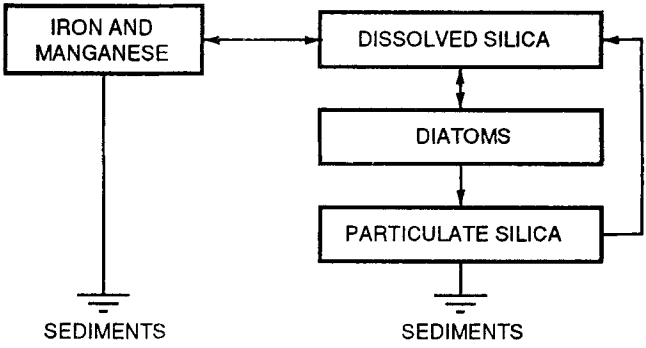

FIG. 4. Simulated Silica Cycle

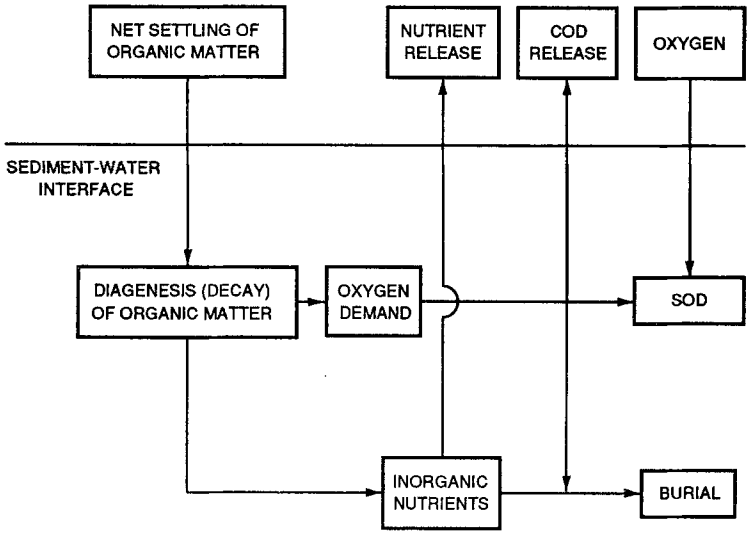

FIG. 5. Diagenetic Sediment Model

is included based on observations that sorption and subsequent settling remove phosphorus from the water column during autumn reaeration events.

In the simulated silica cycle (Fig. 4), dissolved silica is incorporated by diatoms and released to the water column, through predation and mortality, as DSil or particulate biogenic silica (PBS). The PBS undergoes dissolution in the water column or else settles into the benthic sediments along with the silica bound in the biomass of settling diatoms. As with PO_4, DSil also adsorbs to iron and manganese particles, providing a vehicle for removal of DSil from the water column.

The remaining cycle in the model is the dissolved-oxygen (DO) balance. Sources of DO include algal photosynthesis and atmospheric reaeration. DO is lost through algal and heterotrophic respiration, nitrification, and exertion of chemical oxygen demand (COD) released from the sediments.

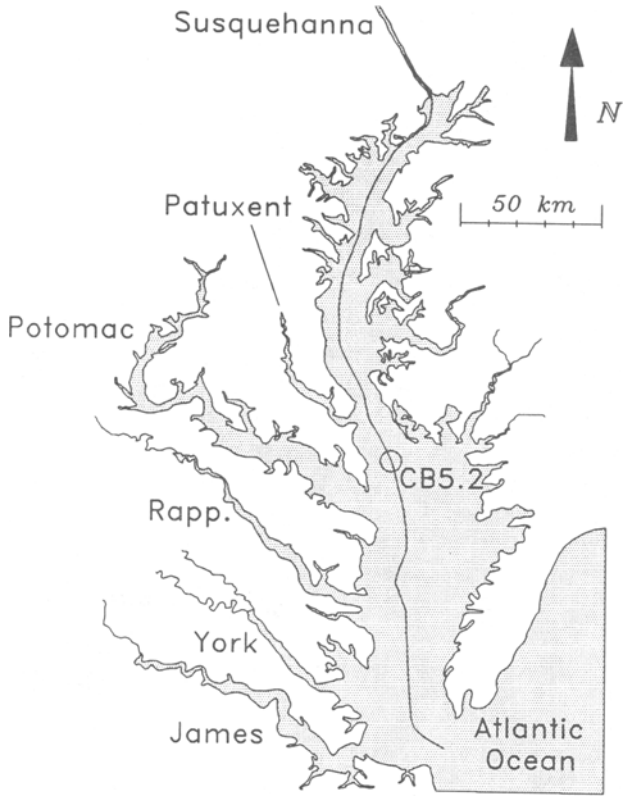

FIG. 6. Chesapeake Bay with Locations of Time-Series and Longitudinal Model-Data Comparisons Shown by Circle and Heavy Line

Sediment Processes

The water-quality model is directly coupled to a predictive benthic-sediment model (Fig. 5). The sediment model (Di Toro and Fitzpatrick 1993) is an expansion of diagenetic principles established for freshwater sediments (Di Toro et al. 1990) into the estuarine environment. CE-QUAL-ICM simulates the settling of particulate matter to the sediments. Diagenesis of accumulated organic matter is computed within the sediment model. The oxygen demand created by carbon diagenesis is fractionated into sediment oxygen demand (SOD), COD release to the water column, and loss through burial. The NH_4 produced by nitrogen diagenesis is routed into three pathways: recycle to the water column, conversion to gaseous nitrogen through coupled nitrification-denitrification reactions, and burial. The actions of nitrification-denitrification also determine sediment-water fluxes of NO_3. The PO_4 produced by phosphorus diagenesis is recycled to the water column, maintained in the sediment as dissolved and particulate (sorbed) PO_4, or lost through burial. The PBS in the sediments undergoes dissolution to DSil or else is buried. Burial also removes a small fraction of reactive organic matter.

The water quality and sediment models interact on a time scale equal to

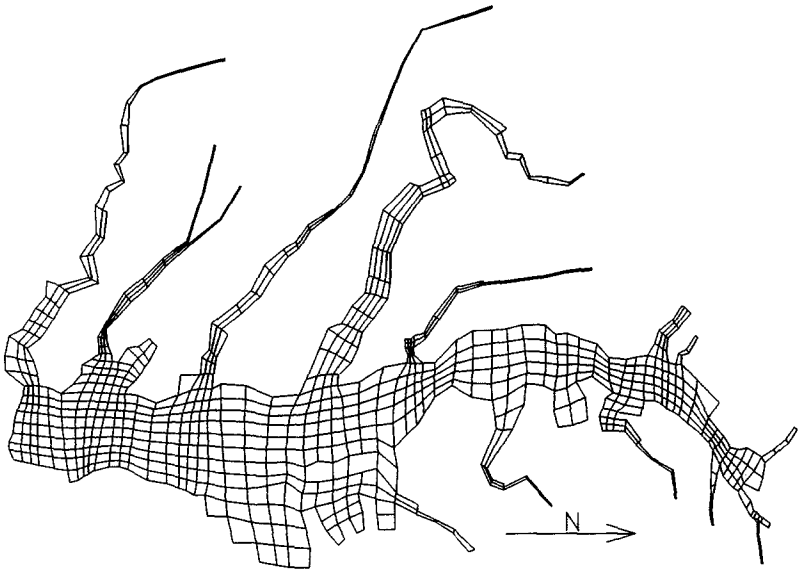

FIG. 7. Boundary-Fitted Computational Grid

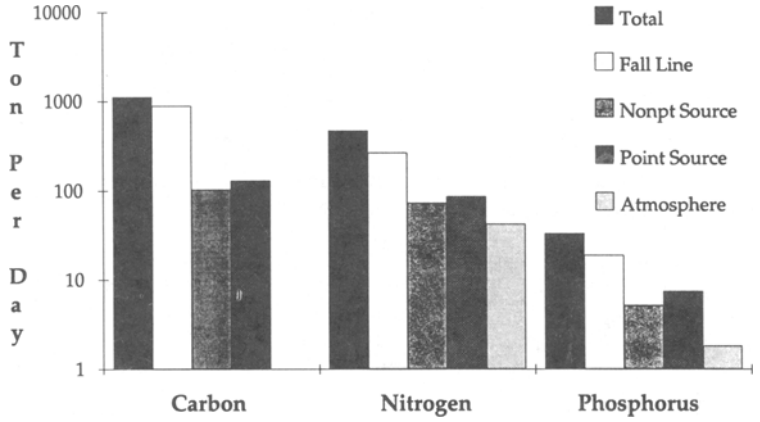

FIG. 8. Mean Carbon, Nitrogen, and Phosphorus Loads to Chesapeake Bay, 1984–86

the integration time step of the water-quality model. After each integration, predicted particle deposition, temperature, and nutrient and dissolved oxygen concentrations are passed from the water-quality model to the sediment model. The sediment model computes sediment-water fluxes of dissolved nutrients and oxygen based on predicted diagenesis and concentrations in the sediments and water. The computed sediment-water fluxes are passed to CE-QUAL-ICM and incorporated into appropriate mass balances and kinetic reactions.

CHESAPEAKE BAY

The Chesapeake Bay system (Fig. 6) consists of the main-stem bay, five major western-shore tributaries, and a host of lesser tributaries and embayments. Urban centers along the bay and tributaries include Norfolk and Richmond, Va., Washington, and Baltimore. The main stem is roughly 300 km long, 8–48 km wide, and 8 m average deep. A trench, up to 50 m deep, traverses the center of the bay. The primary source of freshwater to the system is the Susquehanna River (≈62% of total gauged flow), which empties into the northernmost extent of the bay. Other major sources of freshwater are the Potomac (≈18%) and James River (≈11%). The bay is a partially mixed estuary in which long-term average circulation is upstream along the bottom and downstream near the surface although this pattern is frequently altered by meteorological events.

MODEL APPLICATION

The CBMP operated on a boundary-fitted computational grid containing 729 cells (approximately 10 × 5 km) in the surface plane (Fig. 7). The hydrodynamic and water-quality grids included two to 15 cells, 1.6 m thick, in the vertical for a total of 4,029. The sediment model operated within a single layer 0.1 m deep. CE-QUAL-ICM was applied to the years 1984–86. A continuous integration employing intertidal hydrodynamics and 2-hour time steps was conducted. The application covered a wide range of hydrologic conditions. In 1984, annual flow at the Susquehanna fall line exceeded 90% of the years on record. At the other extreme, 1985 flow was less than 80% of the recorded years. Flow in 1986 was near average, exceeding 60% of the years on record.

External loads to the system were divided into four classes: fall-line loads from the Susquehanna and major tributaries, non–point-source loads that enter the system below the river fall lines, point-source loads from municipal and industrial sources adjacent to the bay and tributaries, and atmospheric loads carried by rain and wind directly to the water surface. Fall-line and non–point-source loads of carbon, nitrogen, and phosphorus were generated by the EPA's Phase II Chesapeake Bay watershed model (Donigian et al. 1991) and input to the model on a 14 day or monthly basis. Point-source loads were provided by regulatory agencies and input to the model on a monthly basis. Seasonal estimates of atmospheric loads were based on NADP observations (*National* 1989) and U.S. EPA estimates (*Chesapeake* 1982).

The magnitude of total loads to the bay varied from year to year but the relative significance of load sources was consistent (Fig. 8). The fall lines were the largest external source of nutrients and carbon to the system. Point-source and non–point-source loads were roughly equivalent but individually much less than fall-line loads. Atmospheric nutrient loads were the least of identified sources.

The primary data base for model calibration and performance evaluation was provided by the EPA's Chesapeake Bay Monitoring Program. The program conducted 20 surveys per year at approximately 90 stations in the main-stem bay and five major tributaries. Over 190,000 observations, in the main stem alone, were processed for comparison with model results.

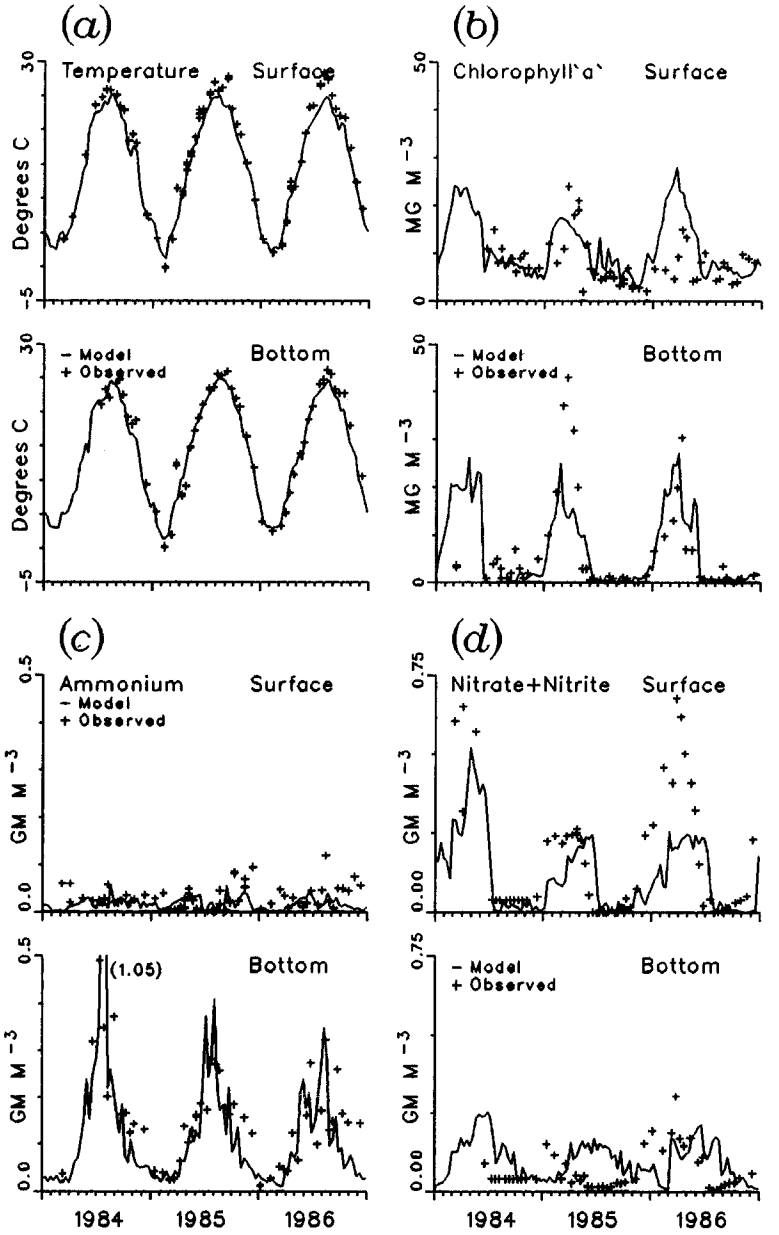

FIG. 9. Time-Series Comparisons of Simulated and Observed: (*a*) Temperature; (*b*) Chlorophyll a; (*c*) Ammonium; (*d*) Nitrate + Nitrite; (*e*) Dissolved Inorganic Phosphorus; (*f*) Dissolved Oxygen; (*g*) Dissolved Silica (Comparisons Are Shown for Data Collected 1 m below Surface and 1 m off Bottom at Station CB5.2)

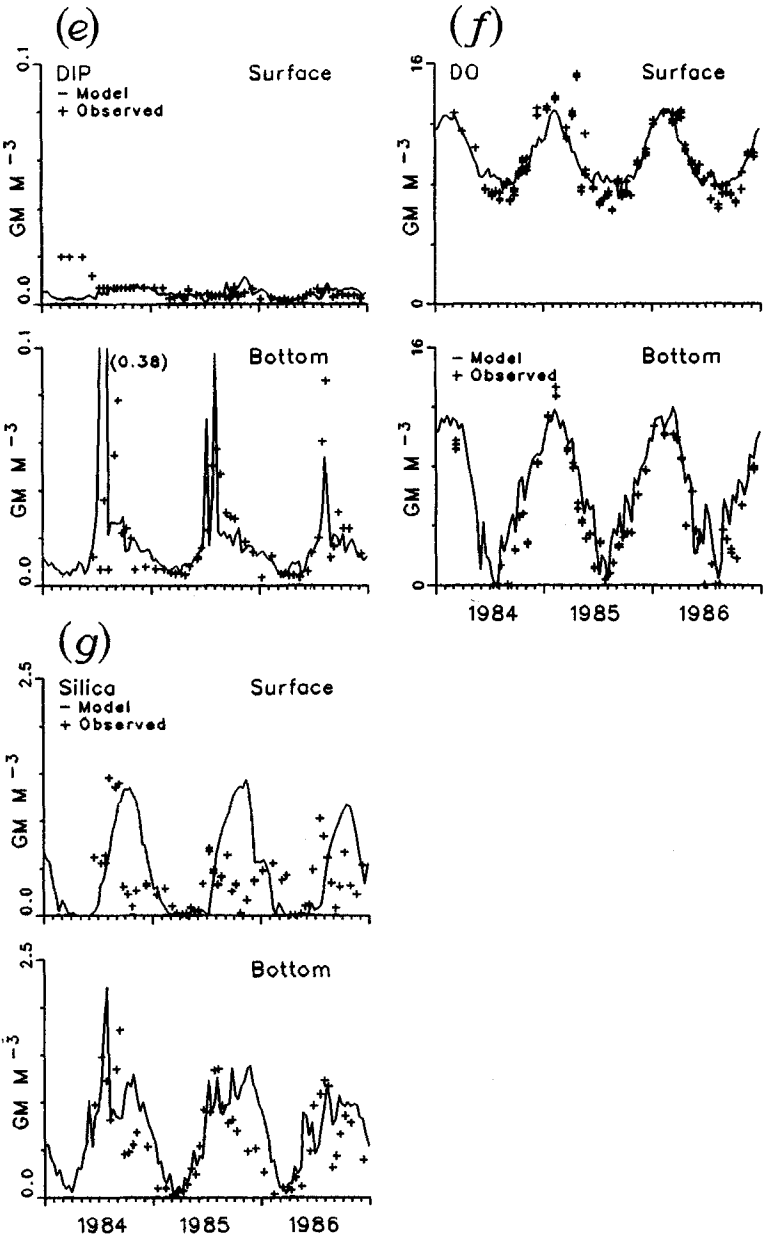

FIG. 9. (*Continued*)

CALIBRATION RESULTS

To calibrate the water-quality model, predictions and observations for the main-stem bay and the major western tributaries were compared in a variety of formats and on several spatial and temporal scales. Only a sam-

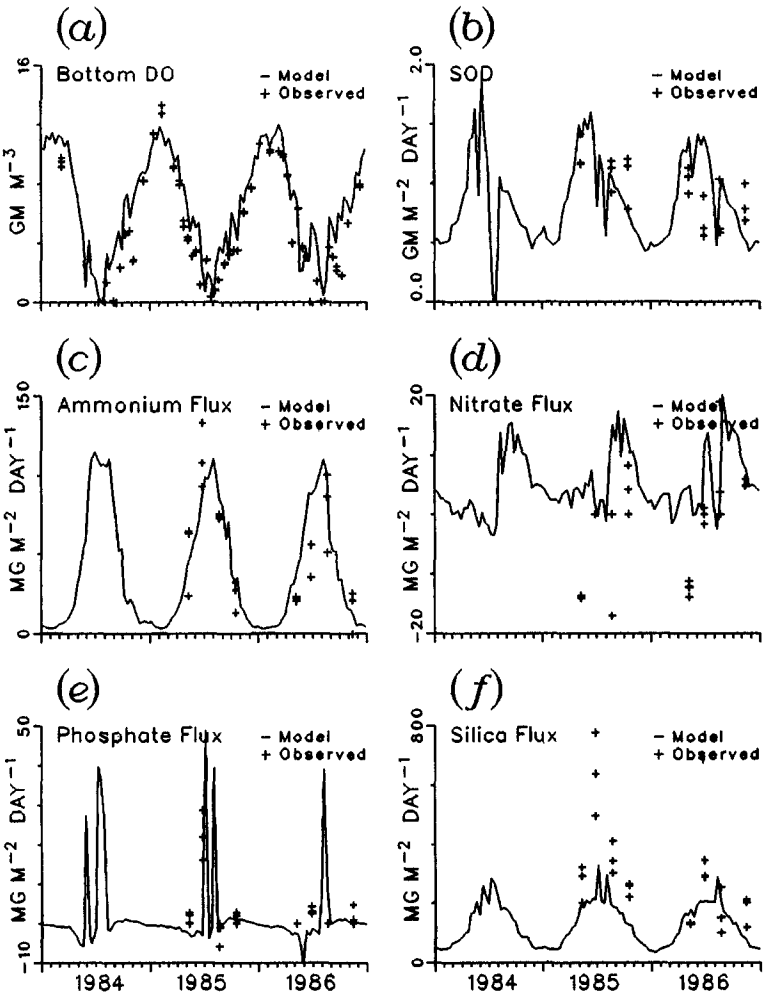

FIG. 10. Time-Series Comparisons of Simulated and Observed: (*a*) Dissolved Oxygen; (*b*) Sediment Oxygen Demand; (*c*) Sediment-Water Fluxes of Ammonium; (*d*) Nitrate; (e) Dissolved Inorganic Phosphorus; (*f*) Silica (Observations Collected at Station CB5.2)

pling of results, selected to illustrate characteristic bay conditions, are shown here. These include 3-year time series of water quality and sediment-water fluxes at midbay, axial distribution of water quality parameters during summer, and spatial distribution of DO in bottom water.

Seasonal Cycling of Chlorophyll, Nutrients, and Dissolved Oxygen

During January, the water column at midbay (Fig. 6) is characterized by low chlorophyll concentration and saturated DO (Fig. 9). Sediment activity is minimal (Fig. 10). Late winter (February–March) is characterized by elevated concentrations of nutrients, especially NO_3, borne by spring runoff

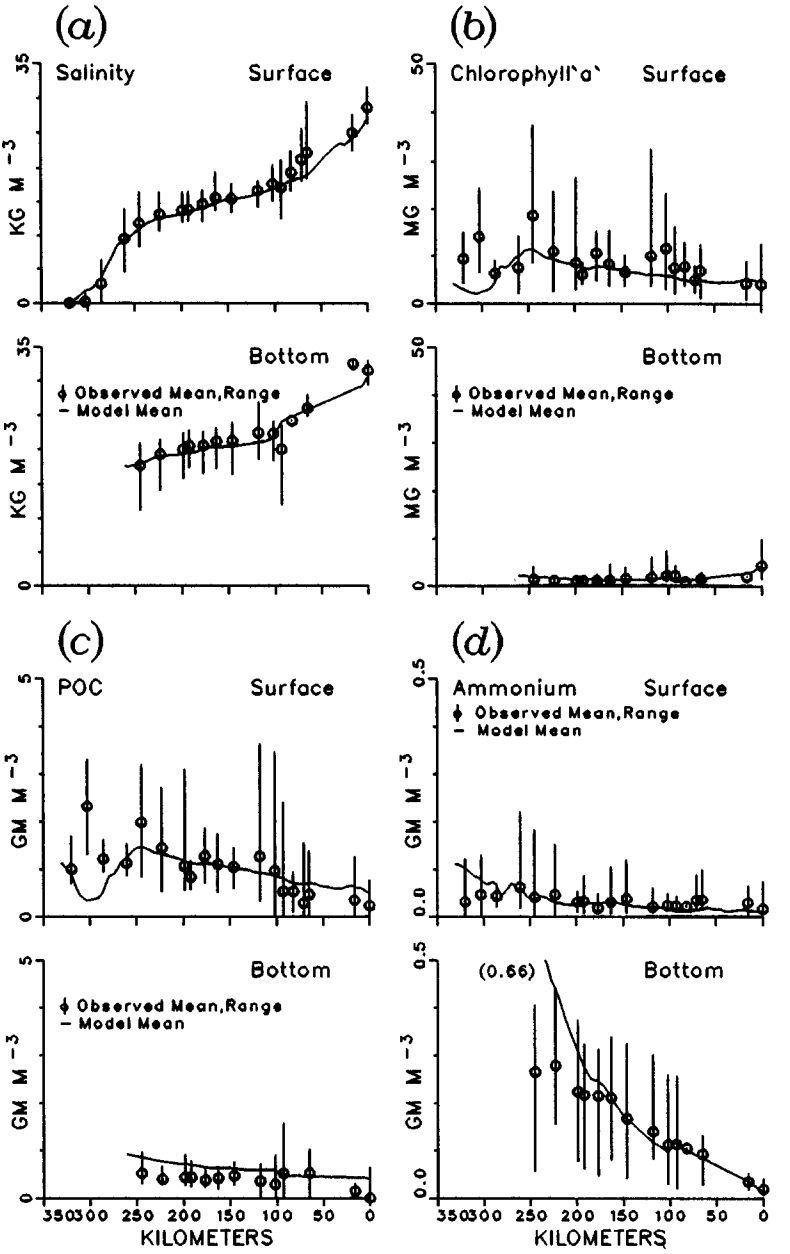

FIG. 11. Longitudinal Comparisons of Simulated and Observed: (*a*) Salinity; (*b*) Chlorophyll a; (*c*) Particulate Organic Carbon; (*d*) Ammonium; (*e*) Nitrate + Nitrite; (*f*) Total Nitrogen; (*g*) Dissolved Inorganic Phosphorus; (*h*) Total Phosphorus; (*i*) Dissolved Oxygen (Predictions and Observations Are Averaged Temporally, June–September 1986, and into Two Layers: Surface 0–6.7 m and Bottom >13 m)

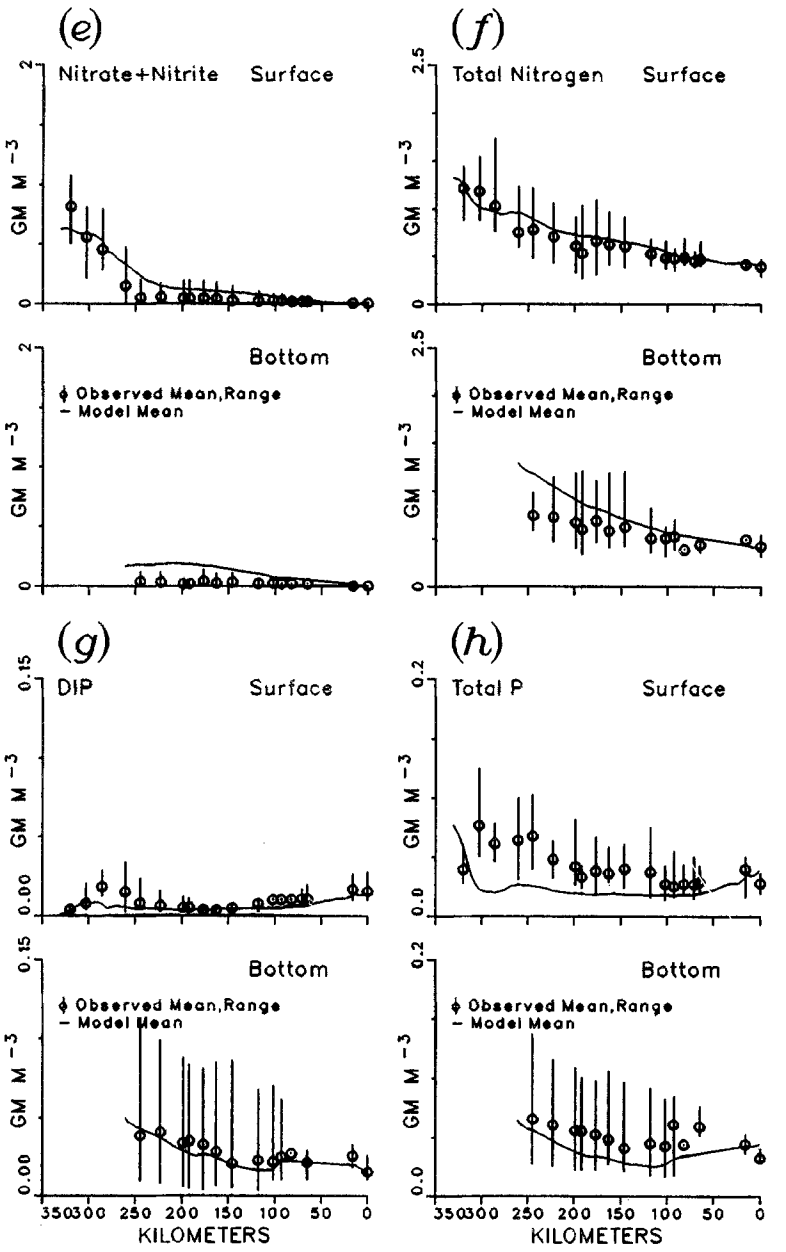

FIG. 11. (*Continued*)

events. These nutrients, especially PO_4 and silica, are rapidly depleted by the spring diatom bloom during which surface and subsurface chlorophyll concentrations attain their annual maxima. Cessation of the bloom and elevated water temperature usher in the summer. By June 1, sediment oxygen demand, spurred by enhanced temperature and deposition of organic

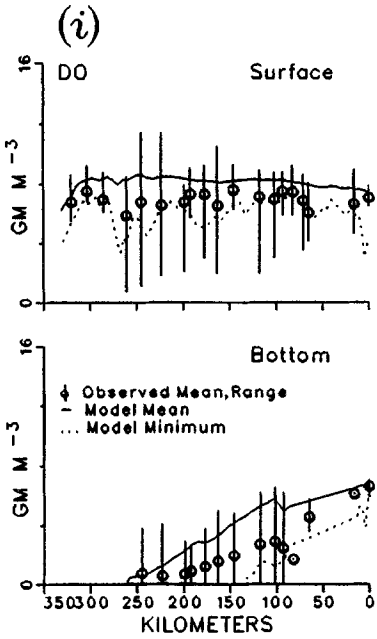

FIG. 11. (*Continued*)

carbon produced in the spring bloom, depletes overlying water of oxygen. Bottom-water anoxia, characteristic of the bay in summer, induces sediment NH_4 and PO_4 release. The NH_4 release is due to inhibition of nitrification within the sediments. Sediment NH_4, which is nitrified to NO_3 and subsequently denitrified to gaseous nitrogen under oxic conditions, is instead released to the water column. PO_4 release occurs because iron oxides in surficial sediments, which adsorb PO_4 and prevent its release under oxic conditions, are reduced to soluble forms allowing free diffusion of sediment PO_4 to overlying water. Temperature-enhanced diagenesis and elimination of sorption capacity also produce summer maxima in silica release. Despite the sediment source of nutrients and immense concentrations of NH_4 and PO_4 in bottom waters, surficial concentrations of NH_4, NO_3, and PO_4 are minimal during summer due to algal uptake. Low-oxygen conditions prevail until autumn climatic conditions cool the water and induce overturn, which mixes oxygenated surface water to the bottom. Reduced temperature diminishes diagenesis; oxygenated water inhibits nutrient releases. As a result, sediment oxygen demand and nutrient releases tend toward their winter minimum values. In the absence of sediment release, nutrient concentrations in bottom waters diminish. Reduced oxygen demand in the water and sediments, coupled with increased vertical mixing, allow DO to increase toward winter saturation concentrations. The bay returns to the state that existed before the nutrient runoff and diatom bloom of the previous spring.

Longitudinal Distribution of Major Constituents

Summer is a critical season for bay water quality due to the occurrence of bottom-water anoxia. Performance of the CBMP during this season was crucial in the evaluation of overall performance. Summer-average predic-

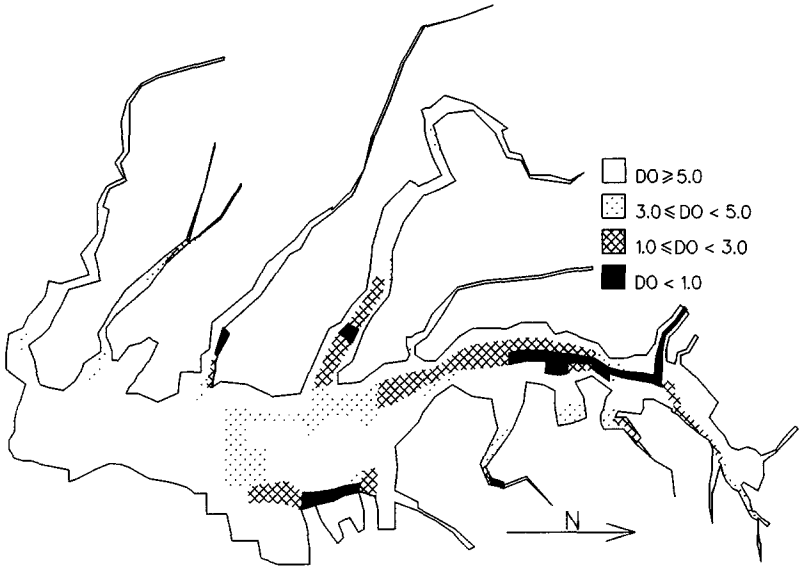

FIG. 12. Simulated Bottom Dissolved Oxygen, June–September 1986

TABLE 2. Mean and Relative Errors

Element (1)	Mean error ($g \cdot m^{-3}$)[a] (2)	Relative error (%) (3)
Chlorophyll a	−1.27	45.8
Particulate organic carbon	−0.17	56.4
Ammonium	−0.007	54.7
Nitrate + Nitrate	0.029	40.2
Phosphate	0.0	38.8
Total phosphorus	0.018	37.8
Dissolved oxygen	−0.479	14.4
Dissolved silica	−0.127	46.5
Total nitrogen	0.042	18.8

[a]Chlorophyll a in $mg \cdot m^{-3}$

tions and observations along the main bay axis (Fig. 6) are shown here for an average hydrologic year (June–September 1986).

During summer, saltwater (Fig. 11) intrudes from its source at the mouth of the bay (km 0) nearly to the Susquehanna fall line (km 300). The vertical gradient at midbay is 5 ppt from top to bottom.

The Susquehanna is the major source of nutrients to the upper bay. Algal growth near this source is inhibited, however, by light extinction associated with the turbidity maximum that occurs at the limit of salt intrusion. Maximum algal concentration occurs downstream of the turbidity maximum at a location where light is sufficient for algal production and nutrients have not been depleted. Particulate organic carbon, produced largely through

TABLE 3. Revisions to Calibration

Date (1)	Total computer runs (2)	Status (3)
December 1990	100	Initial calibration
—	—	Fall-line loads from regression model
April 1991	150	Revised parameter values
—	—	Fall-line loads from regression model
—	—	Revised formulation of boundary conditions
December 1991	200	Revised parameter values
—	—	Fall-line loads from EPA Watershed Model
—	—	Original boundary condition formulation
February 1992	222	Revised parameter values
—	—	Revisions to sediment model
—	—	Fall-line loads from EPA Watershed Model
—	—	Revised formulation of boundary conditions

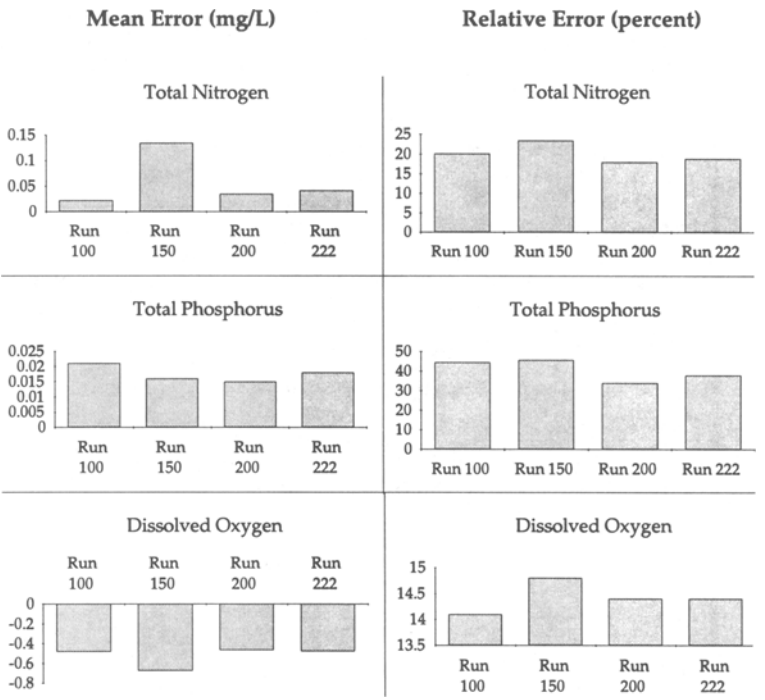

FIG. 13. Mean and Relative Error at Four Stages of Model Calibration

algal primary production, follows the trend of chlorophyll throughout the bay.

Ammonium is largely depleted in surface waters but attains high concentrations in bottom waters near the sediment source. Like NH_4, nitrate ex-

hibits a declining trend from away from high concentration near a source. The trend is longitudinal, however, away form the source at the Susquehanna River. The distribution of total nitrogen is characterized, as well, by a gradient from the source at the Susquehanna to the sink represented by the ocean.

Observed and simulated phosphate mimic NH_4 in that surface waters are depleted by algae, while bottom waters are enriched by sediment release. Observed total phosphorus exhibits a sag with elevated concentrations at both ends of the bay and lower concentrations in the central bay. In the upper bay, the concentration peak consists of particulate phosphorus trapped in the turbidity maximum. In the lower bay, higher concentrations represent phosphorus transported into the bay from the continental shelf. Simulated total phosphorus is less than observed and does not fully replicate the spatial trend. We believe the underestimation of total phosphorus is due to omission of phosphorus loads from bank erosion. The contribution from bank erosion has been estimated as 6,000 kg day^{-1} ("1990 Progress" 1991), roughly 18% of the loads considered in the model package. To completely capture the spatial trend, suspended sediments must be added to the model and phosphate exchange with these solids must be considered.

Surface DO is near saturation everywhere. At the bottom, however, observed DO exhibits a minimum, with average concentration near zero, from km 250, at the head of the trench that runs up the main stem, down to km 200. Intermittent anoxia extends another 100 km down the bay.

Spatial Distribution of Dissolved Oxygen

Regions of anoxia and hypoxia occur almost exclusively below the pycnocline at ≈6 m. Our model agrees with observations (Officer et al. 1984) that low-DO waters follow the channel that leads up the main stem (Fig. 12). Strictly anoxic conditions are confined to the head of the trench, directly under the region of highest algal productivity. Our simulations also indicate significant volumes of oxygen-depleted water in a secondary channel that shoals as it approaches the eastern shore, in the lower Rappahannock and Potomac Rivers, and in Baltimore Harbor.

STATISTICAL EXAMINATION OF MODEL RESULTS

Spatial plots and time series present limited comparisons of predictions and observations. Statistical summaries provide useful information not available in graphical form. Two of the most useful statistics are mean error:

$$ME = \frac{\sum (O - P)}{N} \quad \ldots\ldots (2)$$

and relative error:

$$RE = \frac{\sum |O - P|}{\sum O} \quad \ldots\ldots (3)$$

in which ME = mean error; RE = relative error; O = observation; P = prediction; and N = number of observations. The ME describes whether the model overestimates or underestimates the data. The RE represents the average difference between predictions and observations, normalized by the magnitude of the observations.

Performance statistics were calculated on several time and space scales.

Statistics in Table 2 are for aggregations of the model and data into zones ≈40 km long and extending across the bay, into levels ≈6 m thick, and into four seasons per year.

COMMENTS

The statistics indicate a robust calibration was achieved. The model went through four major phases of calibration (Table 3). In each phase, modifications were made to the computer code, pollutant loads, or parameter values. Although each change produced qualitative improvements in model-data agreement or in predictive power of the model, statistical behavior of several key constituents was largely unchanged from the initial calibration (Fig. 13). Mean errors of total nitrogen, total phosphorus, and DO retained their original biases throughout the calibration period. No monotonic decline in magnitude of mean or relative error was apparent for these constituents. The influence of parameter adjustments and minor model modifications on these constituents was limited.

The insensitivity of several error statistics to calibration exercises is a significant outcome of the CE-QUAL-ICM application to Chesapeake Bay. One accusation commonly leveled at models requiring evaluation of numerous parameters is that data can be infallibly matched through a curve-fitting exercise. In the CBMP, however, predictions are robust and not readily manipulated by the modeler. No amount of parameter adjustment can compensate for deficiencies in formulation or in loading and other forcing functions. Several degrees of freedom traditionally available to calibrate eutrophication models have been eliminated from the CBMP. Lagrangian averaging of three-dimensional hydrodynamics eliminates the use of a dispersion parameter to adjust mass transport. The sediment model eliminates tuning of sediment-water material fluxes. Employment of organic carbon as a state variable, instead of BOD, eliminates approximation of BOD production by algae and extrapolation of short-term to long-term BOD measures.

The progress of statistics through 222 model runs indicates that additional calibration of the model is not warranted at this time. Improvements in model-data agreement require new estimates of loads to the system and/or reformulation of model principles.

CONCLUSIONS

The present study advances the state of the art in eutrophication modeling in three aspects. The first is coupling of the eutrophication model to a three-dimensional time-variable hydrodynamic model. The hydrodynamic and eutrophication models operate on a grid that provides ample lateral and vertical resolution in the main-stem bay and in the lower tributaries. The hydrodynamic model and Lagrangian postprocessor were subject to extensive documentation and peer review and performed to a high degree of accuracy. No modification or tuning of transport to improve performance of the eutrophication model was conducted. Confidence in the accuracy of the hydrodynamics meant that transport was eliminated as an origin of model-data discrepancies in the eutrophication component of the model package.

The second advance is coupling of the eutrophication model with a fully predictive sediment oxygen demand and nutrient flux model. Prior to application of this model package, SOD and nutrient fluxes were commonly

adjusted, perhaps within a range of observations, to optimize agreement of predictions and observations in the water column. This adjustment process has been eliminated. Coupling of the two models places stringent demands on each of them. The eutrophication model must provide correct spatial and temporal deposition of organic carbon, nitrogen, phosphorus and silica to the sediments to fuel diagenesis. Dissolved oxygen and nutrient concentration in the water must be modeled sufficiently to express the effects of DO and nutrients on sediment fluxes. Within the sediment model, the magnitude and temporal phasing of diagenesis and fluxes must be represented accurately to provide the sediment contribution to bottom-water anoxia and nutrient concentrations that characterize the bay in summer.

The third advance is continuous, multiyear application of the model on an intertidal time scale. Prior to application of this model, estuarine eutrophication models were commonly run in steady-state or in a time-variable mode for one season only. Continuous, multiyear application now allows representation of the influence of processes in one season on results in another. For example, the sequence in which nutrients in spring runoff are incorporated into the spring algae bloom, deposited on the bottom, and released during summer is modeled. Multiyear application allows carry-over to subsequent years of organic matter deposited in the sediments. Continuous, multiyear application means the model is available to examine effects of seasonal nutrient control strategies and that estimates of the time for the bay to respond to management activities are now possible.

ACKNOWLEDGMENTS

Development of the Chesapeake Bay model package was sponsored by the U.S. Army Engineer District, Baltimore, and the Chesapeake Bay Program Office, U.S. Environmental Protection Agency. Permission was granted by the Chief of Engineers to publish this information.

APPENDIX I. REFERENCES

Cerco, C., and Cole, T. (1993). *Application of the three-dimensional eutrophication model CE-QUAL-ICM to Chesapeake Bay*. U.S. Army Engineer Waterways Experiment Station, Vicksburg, Miss.

Chesapeake Bay program technical studies, a synthesis. (1982). U.S. Environmental Protection Agency, Washington, D.C., 158–163.

Di Toro, D., Paquin, P., Subburamu, K., and Gruber, D. (1990). "Sediment oxygen demand model: methane and ammonia oxidation." *J. Envir. Engrg.*, ASCE, 116(5), 945–986.

Di Toro, D., and Fitzpatrick, J. (1993). "Chesapeake Bay sediment flux model." *Contract Rep. EL-93-2*. U.S. Army Corps of Engineers Experiment Station, Vicksburg, Miss.

Donigian, A., Bicknell, B., Patwardhan, A., Linker, L., Alegre, D., Chang, C., and Reynolds, R. (1991). *Watershed model application to calculate bay nutrient loadings*. Chesapeake Bay Program Office, U.S. Environmental Protection Agency, Annapolis, Md.

Dortch, M., Chapman, R., and Abt, S. (1992). "Application of three-dimensional Lagrangian residual transport." *J. Hydr. Engrg.*, ASCE, 118(6), 831–848.

Edinger, J., Brady, D., and Geyer, J. (1974). "Heat exchange and transport in the environment." *Rep. 14*, Department of Geography and Environmental Engineering, Johns Hopkins University, Baltimore, Md.

Johnson, B., Kim, K., Heath, R., Hsieh, B., and Butler, L. (1993). "Validation of a three-dimensional hydrodynamic model of Chesapeake Bay." *J. Hydr. Engrg.*, ASCE, 199(1), 2–20.

Leonard, B. (1979). "A stable and accurate convection modeling procedure based on quadratic upstream interpolation." *Comp. Meth. in Appl. Mech. and Engrg.*, 19, 59–98.
National atmospheric deposition program (IR-7)/national trends network. (1989). NADP/NTN Coordination Office, Natural Resources Ecology Laboratory, Colorado State Univ., Fort Collins, Colo.
Officer, C., Biggs, R., Taft, J., Cronin, L., Tyler, M., and Boynton, W. (1984). "Chesapeake Bay anoxia: origin, development, and significance." *Science*, 223, 22–27.
Proceedings of workshop number 1: water column state variables and aquatic processes. (1988). HydroQual Inc., Mahwah, N.J.
"1990 progress report for the baywide nutrient reduction strategy." (1991). *Rep. No. 2*, U.S. EPA Chesapeake Bay Program Office, Annapolis, Md, 41–42.

APPENDIX II. NOTATION

The following symbols are used in this paper:

A_j = area of flow face j;
C_i = concentration in ith compartment;
C_j^* = concentration in flow across flow face j;
Chla = chlorophyll a;
D_j = diffusion coefficient at flow face j;
DO = dissolved oxygen;
DOC = dissolved organic carbon;
DON = dissolved organic nitrogen;
DOP = dissolved organic phosphorus;
Dsil = dissolved silica;
LPOC = labile particulate organic carbon;
LPON = labile particulate organic nitrogen;
LPOP = labile particulate organic phosphorus;
ME = mean error statistic;
N = number of observations;
NH_4 = ammonium;
NO_3 = nitrate + nitrite;
n = number of flow faces attached to ith compartment;
O = observed value;
P = model prediction;
PBS = particulate biogenic silica;
PO_4 = dissolved inorganic phosphorus;
Q_j = volumetric flow across flow face j of ith compartment;
RE = relative error statistic;
RPOC = refractory particulate organic carbon;
RPON = refractory particulate organic nitrogen;
RPOP = refractory particulate organic phosphorus;
S_i = external loads and kinetic sources and sinks in ith compartment;
SOD = sediment oxygen demand;
t = temporal coordinate;
V_i = volume of ith compartment; and
x = spatial coordinate.